# Efficiency Improvement for Motor-Pump Set of a Wind Energy Pumped Storage System Using $V/F^X$ Fuzzy Controller

Muhammad M.A.S. Mahmoud

***Abstract***—In this paper we shall focus on the pump storage systems as an important application for wind energy as the pumped storage systems are more and more involved in renewable energy at high power levels. But at the same time, pumped storage can be successfully used for grid integration of small scale renewable energy sources, such as wind energy. The purpose of this paper is to design optimum fuzzy motor controller for pump driving in order to obtain maximum power available for pumping and minimum motor losses, and hence, a higher efficiency of the pump. Two fuzzy motor controllers based on linear dependency (V/Hz) and cubic dependency ($V/Hz^3$) between voltage and frequency are developed for induction machine in pumped storage applications. The fuzzy controller is designed to receive frequency input from the network and estimate the required firing angle of a full-wave Thyristor circuit placed between the source and the load to control the load voltage. The fuzzy controllers have considered the variation of the power supply frequency during the motor starting and running cases to select the optimum applied voltage to the motor for both cases. Simulation of the motor operation during the starting and running is carried out for the full applicable range of frequency. The results and the detailed graphs show how the designed controller is fast and accurate. Required motor protection and comparison between DC link and Thyristor full wave circuit control has been discussed as well.

***Keywords-***Fuzzy logic, Fuzzy Controller, Motor Control Pumping Storage Fuzzy Control, Motor efficiency improvement.

## I. Introduction

SOURCES of renewable energy, which are more and more promoted in the global warming context, need special requirements for grid connection. Even more delicate issues are to be taken into account when unpredictable and variable energy sources, like wind or solar energy, need to be grid connected [1], [2], [3].

For wind energy, pumped storage is a good alternative to grid connection. When grid connection is not allowed, the supplemental energy obtained in high wind speed periods may be used for pump water from an inferior basin to a superior one, and this water may be released in peak load periods when there is need for energy [4], [5].

In this way, no energy is lost and the grid is not perturbed by unstable energy [6], [7].

On the other hand, pumped storage provides good storage properties: large scale, long time, no toxic materials involved, and no sophisticated and expensive equipment- is necessary [8].

Muhammad M.A.S. Mahmoud is with Al Hosn Gas Co. UAE (phone: +37257-368752; e-mail: mmanar@ieee.com).

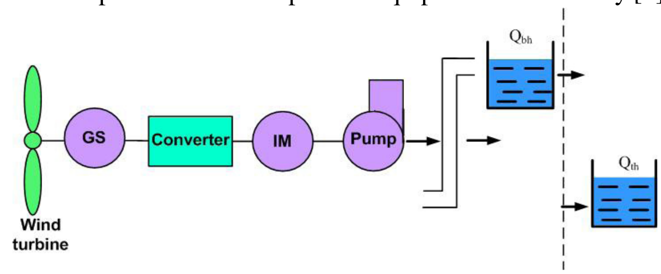


Fig. 1. Wind energy pump storage system

A pumped storage for wind energy looks as figured in Fig. 1. It – consists of wind turbine, generator, converter, motor for driving pump and pump.

According to the distance from the storage lake and the wind generator the energy source can be connected to the utilities grid or work autonomously when the distance is less than 20 km [3]

The disadvantage of pumped storage for autonomous renewable energy sources is small global efficiency [9], because of the many components involved in the electro-energetic chain. The efficiency of a system is defined as the ratio between input and output power. For wind energy pumped storage system, the global efficiency is the ratio of the power given by the wind turbine generator and the power available for pumping. However, an optimized operation of the storage system is obtained taken part by part from all the elements of the electro-energetic chain of the wind energy pumped storage system to improve efficiency.

In [10], motor control concept for driving a pump was discussed in order to obtain maximum power available and a higher efficiency of the pumping system using DC link Converter. Open-loop Controller was used to obtain the results. However, in this paper we shall develop the required close-loop voltage- frequency dependency controller using a simple full-wave Thyristor circuit, whose firing angle is tuned by fuzzy logic controller (Fig. 2). The results shall be illustrated and discussed hereinafter.

## II. System Modeling

### A. Power supply:

The wind turbine and its induction generator are modeled as simple variable frequency power supply with constant phase voltage of 400Volt. The power supply is connected to the load through full-wave Thyristor circuit.

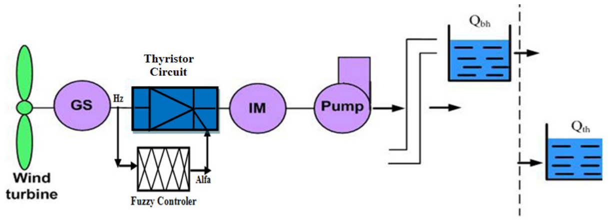


Fig. 2. Wind energy pump storage system with voltage- frequency dependency fuzzy controller

*B. Motor:*

The motor load is modelled as 5.5kW induction motor with the following parameters:

1) Nominal Apparent Power = 6.962 VA, Line to line Voltage = 380V, Frequency = 50Hz
2) Stator Resistance = 0.71 Ohm, Stator Inductance = 4.5 mH
3) Rotator Resistance = 0.728 Ohm, Rotator Inductance = 4.5 mH
4) Mutual Inductance: 93.75 mH
5) Inertia = 0.2, kg.m^2, Friction Factor = 0.051 N.m.s, Pole pairs = 3

*C. Pump:*

The pump load has been modeled by the following Speed/Torque and respective Speed/Power curves:

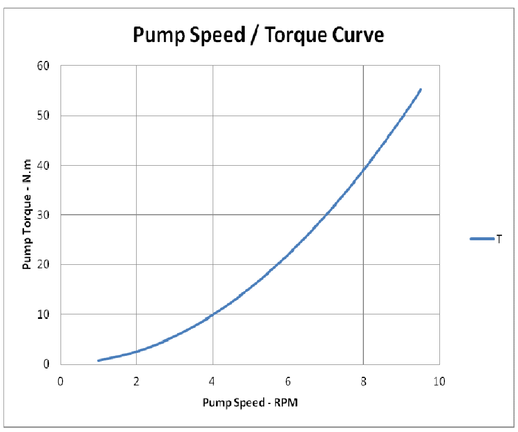


Fig 3. Pump Speed/Torque

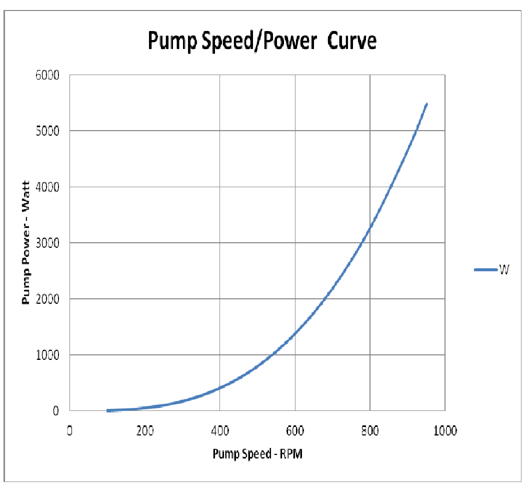


Fig 4. Pump Speed/Power

The optimum voltage frequency dependant characteristic has been analyzed in[10], for the maximum efficiency. The analyses recommended the following characteristics for starting and running cases:

*D. Starting characteristic:*

Motor starting was made on V/Hz characteristic with slope 30/5.

*E. Running characteristic:*

1) In the range of 5 Hz and 10 Hz, it was imposed on the motor to go on the characteristic determinate from the motor datasheet, which is:

$$V/\,Hz_1^{\,3} = 0.0025\ 3.\ f^3 + 30. \qquad (1)$$

2) In the range of 10 Hz and 20 Hz the motor was imposed to pass on characteristic given by:

$$V/\,Hz_2^{\,3} = 0.005\ 3.\ f^3 + U_{10Hz}. \qquad (2)$$

3) In the range of 21 Hz and 25 Hz, motor was imposed to pass on characteristic:

$$V/\,Hz_3^{\,3} = 0.006\ 3.\ f^3 + U_{20Hz}. \qquad (3)$$

4) Above 25Hz, the characteristic was based on

$$V/\,Hz_2^{\,3} = 0.0025.\ f^3 + U_{25Hz} \qquad (4)$$

in parallel with:

$$V/\,Hz_1^{\,3} = 0.0025\ 3.\ f^3 + 30 \qquad (5)$$

(Determined from datasheet values).

Where:

$U_{10Hz}$, $U_{20Hz}$ and $U_{25Hz}$ represents the voltage at 10 Hz, 20 Hz and 25 Hz respectively.

The optimum voltage-frequency characteristic for the maximum efficiency illustrated in Fig. 5.

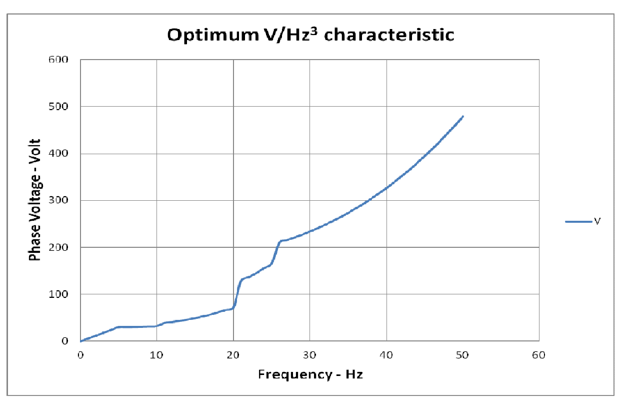


Fig 5. Optimum V/H3 Characteristic.

*F. Controller:*

In order to build fuzzy controller with input signal "frequency" and output signal "firing angle-Alfa" to tune the the motor applied voltage to the corresponding input signal frequency based on the optimum voltage-frequency characteristic for the maximum efficiency, it is important to develop a direct relation between "firing angle-Alfa" and the frequency based on the optimum voltage-frequency characteristic.

1) Step 1:

The effect of single-phase full-wave circuit is considered to determine the size load voltage and current at different firing angle "Alfa". The general formulas for the r.m.s values of the current ($I_{load}$) and the voltage ($V_{load}$) across a load, comprise of inductance in series with resistance, controlled by single-phase full-wave circuit are given in [11]. These formulas are as follows:

$$I_{Load} = \frac{\sqrt{2}\times V_{source}}{z}\left[\frac{1}{\pi}\int_{\pi}^{\beta}\{\sin(\omega t-\theta)-\sin(\alpha-\theta)e^{(r/l)(\alpha/\omega - t)}\}d\omega t\right]^{1/2} \quad (6)$$

$$V_{Load} = V_{source}\left[\frac{1}{\pi}\left(\beta-\alpha+\frac{\sin(2\alpha)}{2}-\frac{\sin(2\beta)}{2}\right)\right]^{1/2} \quad (7)$$

Where:

$\omega = 2\pi$ f radian/second

$\alpha$ (Alfa)= Firing angle

$\beta$ = Extinction angle (cut-off angle)

$\theta$ = tan-1 ( l/ r)

l = Load Inductance

r = Load Resistance

t = Time

z = Load impedance.

Since the conducting angle $\delta = \beta - \alpha$ cannot exceed $\pi$, then the firing angle $\alpha$ will not be less than $\theta$ and hence the control range of the firing angle is

$$\pi \geq \alpha \geq \theta \quad (8)$$

To maximize the firing angle range for better voltage control, a resistive load may be inserted in parallel to the motor to minimize the value of $\theta \cong 0$.

For maximum power transferred to the motor, the maximum conducting angle is considered. Therefore, the value of the controlled voltage corresponding to each firing angle $\alpha$ can be calculated assuming that $\alpha = \pi/2$ and $\beta = \pi$

The value of the controlled voltage with respect to firing angle at different frequency values can be found by practical and fast method using the MATLAB Simulink tool [12]. Figure 6 illustrates the proposed model that has been used to evaluate the value of the controlled voltage for different value of firing angels $\alpha$ (Alfa).

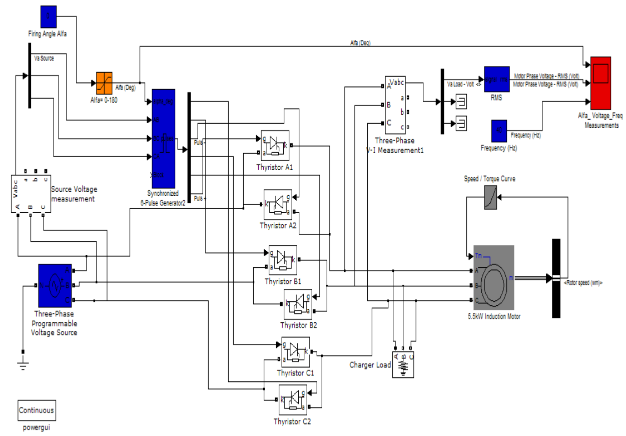


Fig 6. Proposed Model to calculate the controlled voltage for different value of firing angels $\alpha$ (Alfa)

Using the Simulink model shown in Figure 6, direct relations between "firing angle-Alfa" and the "frequency" based on the optimum voltage-frequency characteristic given in section 2.4 and 2.5 are illustrated in the following figures 7 and 8:

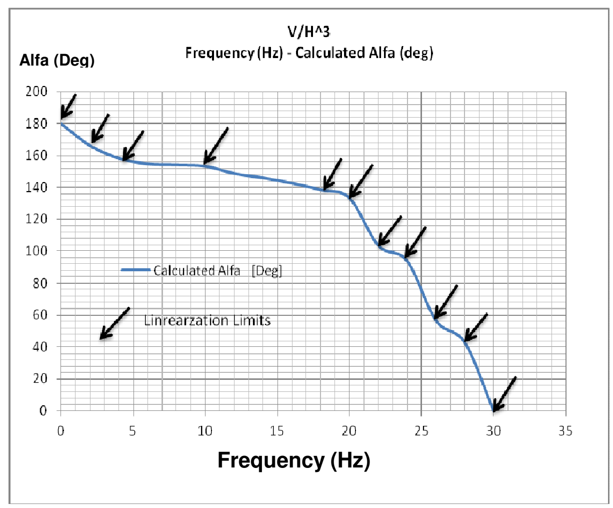


Fig 7 . Relations between "firing angle-Alfa" and the "frequency" based on V/Hz$^3$ Characteristic

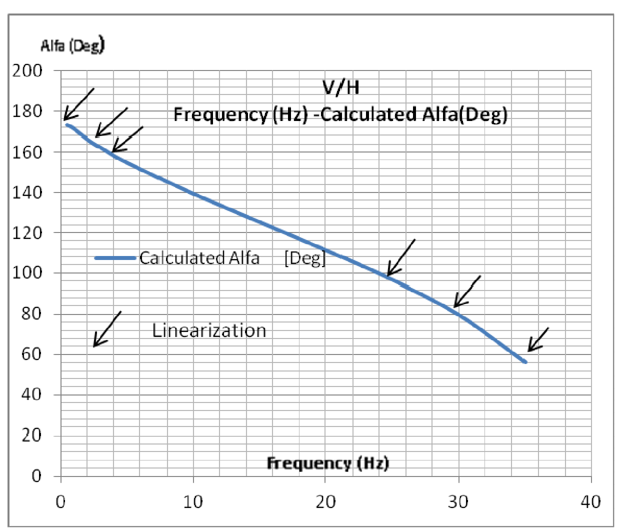


Fig 8 Relations between "firing angle-Alfa" and the "frequency"

based on V/Hz Characteristic.

2) Step 2:

In this step, we shall linearize the “Alfa-Frequency” curves obtained in Step 1.

The resultant curves related to V/H and V/H$^3$ are divided into M and N sections respectively (marked in yellow in the result tables), which can be approximated to the nearest linear sections. Two Fuzzy condolers are built. One for V/Hz$^3$ H “Alfa-Frequency” curve and another one for V/H “Alfa-Frequency” curve. The first Fuzzy Controller consists of M fuzzy sub-controllers, each representing one section, and the second controller consists of N sub-controllers each representing one section as well.

The resultant output of each fuzzy sub-controller will be equal to the respective linearized section using the following functions for fuzzy implication process:

- Mamdany engine.
- Triangle type for Membership functions.
- Product for And.
- Max for Or.
- Min for Implication
- Proportional for Aggregation.
- Largest of Maximum for Defuzzification
- With Fuzzy rule:

IF (Frequency) IS MF(input)$^a$ THEN ($\alpha$) IS MF(output)$^b$ (9)

where,

a = 1,2,…K (fuzzy membership function number)

b = K – a + 1 (fuzzy membership function number)

and K is the number of the fuzzy membership function.

Based on the above fuzzy setup, the following figure illustrates a typical input/output for a fuzzy sub-controller related to V/Hz$^3$ with input frequency range of 28-30 Hz and output firing angle Alfa($\alpha$) range of 0- 42.8 Deg. The results prove the validity of fuzzy sub-controller to represent the linearzed section for this specific range.

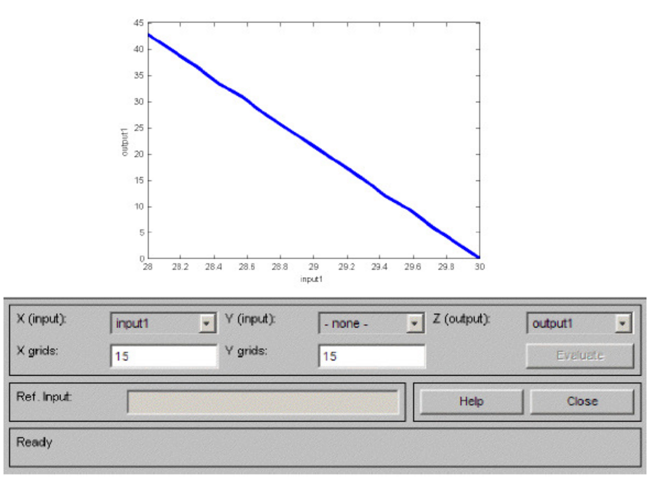


Fig 9: Typical input/output for a fuzzy sub-controller related to V/Hz$^3$

3) Step 3:

Simulink toolbox is used to build V/Hz$^3$ fuzzy controller for the motor-pump system illustrated in Fig 2. Full simulation is carried out to operate the induction motor from frequency range 0-50 Hz. The motor is assumed initially under running condition (Slip = 0.02), as motor starting was made on V/Hz characteristic not on V/Hz$^3$. The result is found as following in Table 1:

TABLE 1: RESULTS OF V/HZ$^3$ FUZZY CONTROLLER FOR THE MOTOR-PUMP SYSTEM

| Source Phase Voltage [V] | Source Frequency [Hz] | Required Controlled Phase Voltage [V] | Calculated Alfa [Deg] | Measured Alfa [Deg] | Measured of Controlled Phase Voltage [Volt] | Measured % Efficiency |
|---|---|---|---|---|---|---|
| 231 | 0 | 0 | 180 | rotor locked | rotor locked | rotor locked |
| 231 | 2 | 12 | 166.4 | rotor locked | rotor locked | rotor locked |
| 231 | 4 | 24 | 158.5 | 158.6 | 23.82 | 11.07 |
| 231 | 6 | 30.54 | 155 | 156 | 26.56 | 29.25 |
| 231 | 8 | 31.28 | 154.3 | 155.2 | 29.59 | 47.27 |
| 231 | 10 | 32.5 | 153.5 | 153.5 | 32.54 | 49.91 |
| 231 | 12 | 41.15 | 148.9 | 149.7 | 39.36 | 55.5 |
| 231 | 14 | 46.22 | 146.2 | 145.8 | 47.07 | 60.38 |
| 231 | 16 | 52.98 | 142.9 | 142.4 | 53.89 | 60.2 |
| 231 | 18 | 61.66 | 138.7 | 138.8 | 61.2 | 64.88 |
| 231 | 20 | 72.5 | 133.5 | 133.5 | 72.49 | 67.59 |
| 231 | 22 | 136.4 | 103.7 | 103.7 | 1363 | 68.66 |
| 231 | 24 | 155.44 | 94 | 94.1 | 155.2 | 70.21 |
| 231 | 26 | 210 | 56.7 | 56.7 | 209.9 | 64.9 |
| 231 | 28 | 221 | 42.8 | 42.8 | 221 | 69.11 |
| 231 | 30 | 233.8 | 0 | 0 | 230.2 | 71.3 |
| 231 | 35 | 233.8 | 0 | 0 | 230.2 | 73.75 |
| 231 | 40 | 233.8 | 0 | 0 | 230.2 | 70.85 |
| 231 | 45 | 233.8 | 0 | 0 | 230.2 | 66.42 |
| 231 | 50 | 233.8 | 0 | 0 | 230.2 | 61.7 |

TABLE 2: RESULTS OF V/HZ FUZZY CONTROLLER FOR THE MOTOR-PUMP SYSTEM

| Source Phase Voltage [V] | Freq [Hz] | Required Controlled Phase Voltage [Volt] | Calculated Alfa [Deg] | Measured Alfa (Deg) | Measured of Controlled Phase Voltage [Volt] | Starting Time [sec] | V/H_SS % Efficiency |
|---|---|---|---|---|---|---|---|
| 231 | 0.5 | 3 | 173.1 | rotor locked | rotor locked | rotor locked | rotor locked |
| 231 | 1 | 6 | 171. | rotor locked | rotor locked | rotor locked | rotor locked |
| 231 | 2 | 12 | 166.3 | rotor locked | rotor locked | rotor locked | rotor locked |
| 231 | 2.8 | 16.8 | 163 | 17.64 | 162.5 | 1.3 | 10.9 |
| 231 | 3 | 18 | 162.5 | 161.8 | 18.53 | 1.2 | 10.3 |
| 231 | 4 | 24 | 158.4 | 158.4 | 24.16 | 1.05 | 10.4 |
| 231 | 5 | 30 | 154.9 | 154.9 | 30.12 | 1 | 14.6 |
| 231 | 10 | 60 | 139.4 | 141.5 | 55.7 | 0.66 | 37 |
| 231 | 15 | 90 | 125.4 | 91.56 | 124.7 | 0.35 | 51.6 |
| 231 | 20 | 120 | 111.5 | 110.2 | 122.9 | 0.22 | 63 |
| 231 | 25 | 150 | 96.8 | 96.8 | 150.1 | 0.138 | 72 |
| 231 | 30 | 180 | 79.9 | 79.9 | 180 | 0.12 | 77 |
| 231 | 35 | 210 | 56.5 | 56.5 | 210.1 | 0.1 | 75 |
| 231 | 40 | 230 | 0 | 0 | 230.2 | 0.12 | 70.9 |
| 231 | 45 | 230 | 0 | 0 | 230.2 | 0.2 | 66.4 |
| 231 | 50 | 230 | 0 | 0 | 230.2 | 0.33 | 61.7 |

4) Step 4:

In this step, Simulink toolbox is used to build V/Hz fuzzy controller instead of $V/Hz^3$. The motor is assumed initially at stand still (Slip =1). The result is summarized in the Table 2.

5) Step 5:

From Step 3 and Step 4, the efficiency at steady state can be compared between $V/Hz^3$ and V/H controller. The result is given in the following Figure10-a&b.

From Figure 10-a, it can be noticed that the maximum efficiency alternates between both controllers. From

Frequency 2.8Hz to 23.5Hz, maximum efficiency can be achieved by $V/Hz^3$ controller. However, from Frequency 23.5 to 37 Hz, maximum efficiency can be achieved by V/Hz controller. For the frequency range greater than 37Hz, the firing angle for both controllers reaches its minimum (zero), and the applied voltage to the motor reaches its maximum value (230 V), therefore, both controllers have the same results for the efficiency. Fig 10-b illustrates the envelopment of the net maximum efficiency achieved by both controllers.

In order to build the required fuzzy controller, following criteria must be considered, as well as to build the controller:

a. The Controller must switch to V/Hz characteristic during the motor starting.

b. For maximum efficiency:
   - The controller must be switched to $V/Hz^3$ for frequency less than 23.5 Hz.
   - The Controller must be switched to V/Hz in the frequency range 23.5Hz to 37Hz.

Figure 11 illustrates the proposed fuzzy controller to achieve the maximum efficiency for the operation of the pump-motor at any frequency.

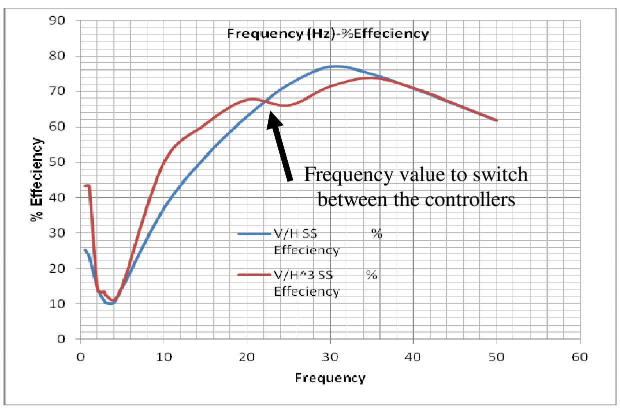


Fig.10-a. Efficiency at steady state achieved by both controllers V/Hz and $V/Hz^3$

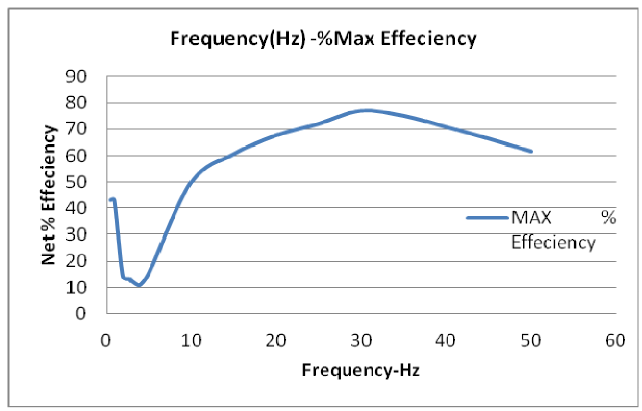


Fig.10-b. Envelopment of the net maximum efficiency achieved by both controllers.

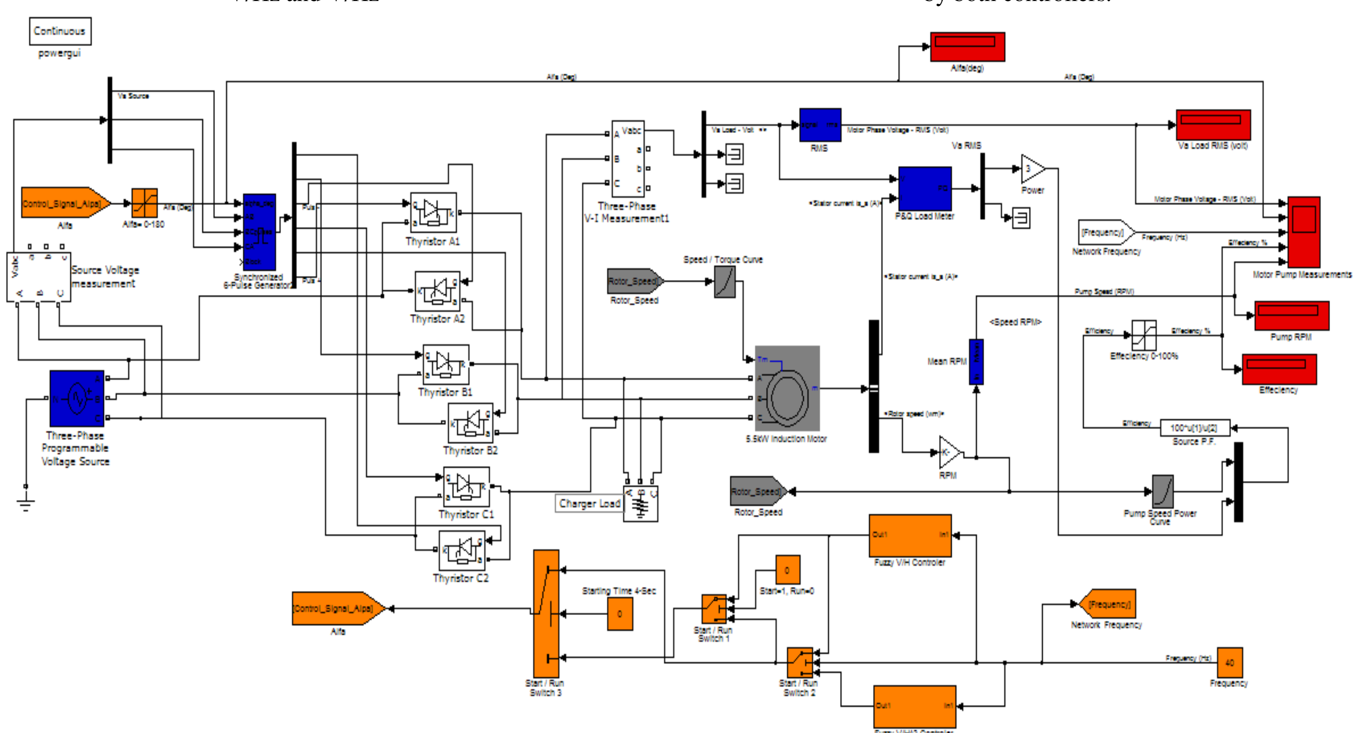


Fig 11: Proposed fuzzy controller to achieve the maximum efficiency for the operation of the pump-motor at any frequency

## III. Results and Disruption

The model has been used to determine the main pump –motor characteristics such as "Efficiency", "Power", "Losses", "Power Factor", "Starting Time" and "Protection", for the effective frequency range from 2.8Hz to 35Hz. The result shall be illustrated and discussed hereinafter in this clause.

### *A. Efficiency:*

Neglecting the losses in the Thyristor circuit, the Input power-efficiency curve obtained by full wave Thyristor circuit controller in this paper can be compared with the result achieved in [10], using DC link controller. Figure 12 illustrates the results:

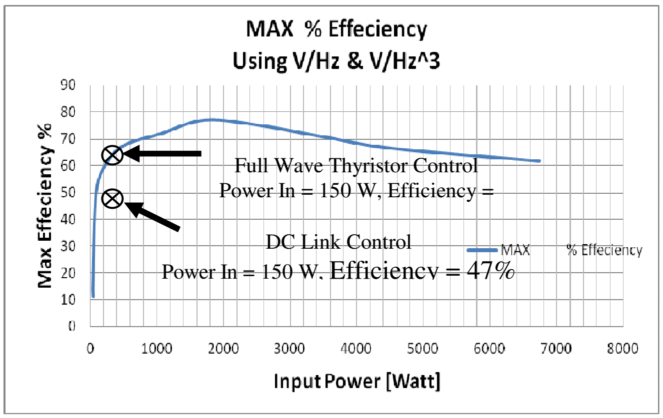


Fig 12. Comparison between Tyristor full wave controller results and DC link controller results

From the result it is noticeable that the at input power of 150 Watt, the efficiency of the pump-motor system has improved from 47% to 64% by using the proposed fuzzy controller to tune the firing angle of full wave Thyristor circuit.

### *B. Power Factor:*

Table 3 illustrates the motor power factor in case of applying V/Hz and V/Hz$^3$ controller. Comparing Table 3 with Figure 10, it can be easily correlate between the two curves to concluded that the maximum efficiency envelop is tracing the maximum power factor obtained from both controllers.

### *C. Power*

"Motor Input Power", "Motor Output power" and "Pump Output power to the Pump are illustrated in Tables 4, 5 and 6 respectively.

For the "Motor Input Power", it is noticeable that in the effective frequency range from 2.8Hz to 35 Hz, controller has operated the motor at minimum power that can be obtained by either V/Hz or V/Hz$^3$. This result is consistent with 2.2 as the motor losses were also minimized due to the improvement of the motor power factor (See Table 7). However, for the "Motor Output Power" curve (Table 5) shows that the less power become available for the pump and consequently the pump has provided less power output for pumping the fluid (Table 6).

Table 3: Motor power factor results

| Freq [Hz] | V/H SS Power Factor | V/H^3 SS Power Factor | MAX % Efficiency |
|---|---|---|---|
| 2.8 | 0.46 | 0.47 | 0.47 |
| 3 | 0.43 | 0.45 | 0.45 |
| 4 | 0.365 | 0.363 | 0.365 |
| 5 | 0.32 | 0.36 | 0.36 |
| 10 | 0.285 | 0.654 | 0.654 |
| 15 | 0.264 | 0.717 | 0.717 |
| 20 | 0.294 | 0.734 | 0.734 |
| 25 | 0.353 | 0.216 | 0.353 |
| 30 | 0.397 | 0.2184 | 0.397 |
| 35 | 0.423 | 0.337 | 0.423 |

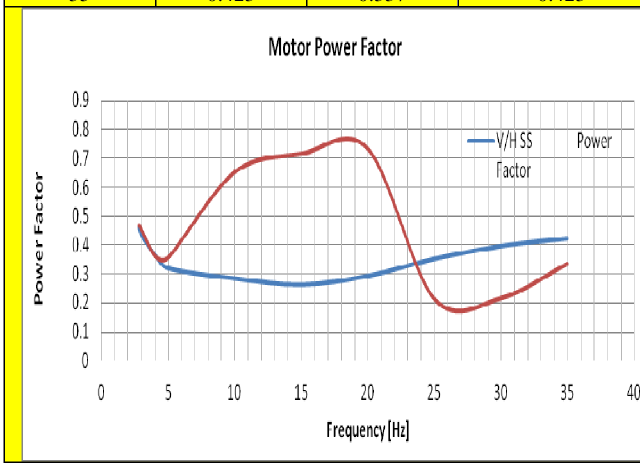


Table 4: Motor Input Power Results

| Freq [Hz] | V/H SS Input Power to the Motor [WATT] | V/H^3 SS Input Power to the Motor [WATT] | MAX % Efficiency |
|---|---|---|---|
| 2.8 | 32 | 27 | 0.47 |
| 3 | 34 | 30 | 0.45 |
| 4 | 46.2 | 44.7 | 0.365 |
| 5 | 60 | 41 | 0.36 |
| 10 | 140 | 86 | 0.654 |
| 15 | 328 | 234 | 0.717 |
| 20 | 617 | 500 | 0.734 |
| 25 | 1059.9 | 1184 | 0.353 |
| 30 | 1716.31 | 1899 | 0.397 |
| 35 | 2536.4 | 2600 | 0.423 |

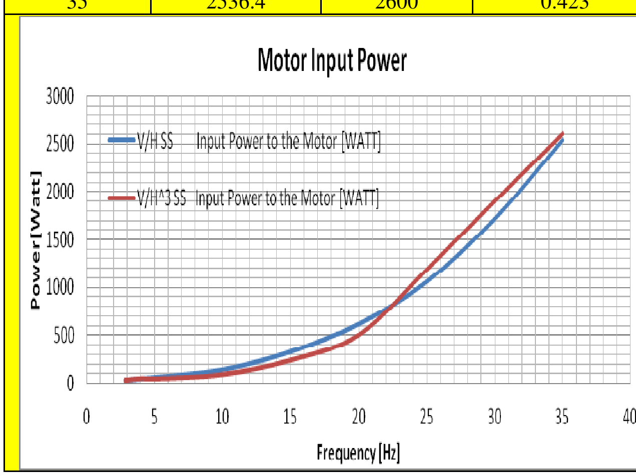

TABLE 5: MOTOR OUTPUT POWER RESULTS

| Freq [Hz] | V/H SS Output Power from the Motor [WATT] | V/H^3 SS Output Power from the Motor [WATT] | MAX % Efficiency |
|---|---|---|---|
| 2.8 | 3.45 | 3.4 | 0.47 |
| 3 | 4 | 3.9 | 0.45 |
| 4 | 7.2 | 7.1 | 0.365 |
| 5 | 11.5 | 11.1 | 0.36 |
| 10 | 70 | 58 | 0.654 |
| 15 | 213 | 178 | 0.717 |
| 20 | 478 | 412 | 0.734 |
| 25 | 896 | 916 | 0.353 |
| 30 | 1504 | 1548 | 0.397 |
| 35 | 2280 | 2305 | 0.423 |

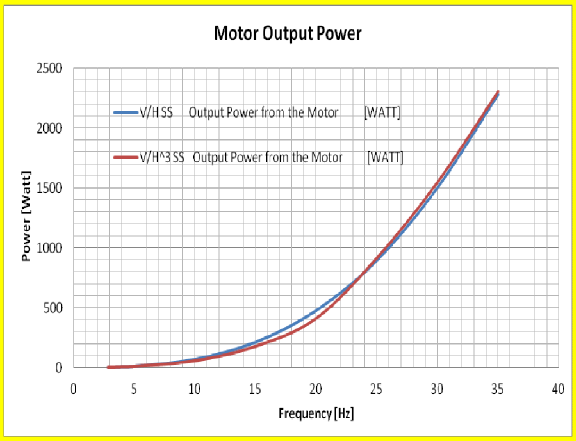


TABLE 6: PUMP OUTPUT POWER RESULTS

| Freq [Hz] | V/H SS Output Power From Pump [WATT] | V/H^3 SS Output Power To Pump [WATT] | MAX % Efficiency |
|---|---|---|---|
| 2.8 | 3.41 | 3.39 | 0.47 |
| 3 | 3.67 | 3.65 | 0.45 |
| 4 | 4.95 | 4.93 | 0.365 |
| 5 | 6.75 | 6.3 | 0.36 |
| 10 | 49 | 43 | 0.654 |
| 15 | 167 | 142 | 0.717 |
| 20 | 393 | 343 | 0.734 |
| 25 | 763 | 781 | 0.353 |
| 30 | 1321 | 1353 | 0.397 |
| 35 | 1897 | 1914 | 0.423 |

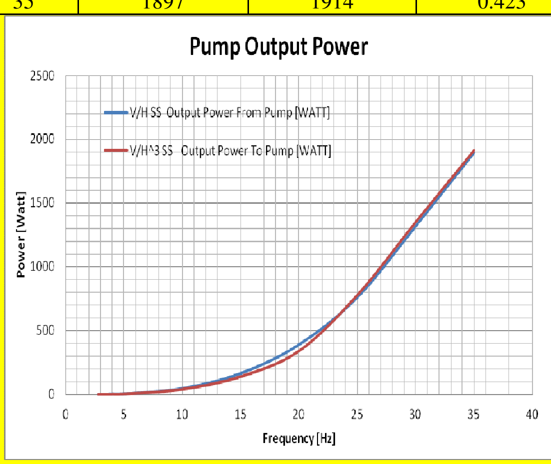


TABLE 7: MOTOR LOSSES RESULTS

| Freq [Hz] | V/H SS Motor Losses [Watt] | V/H^3 SS Motor Torque [Watt] | MAX % Efficiency |
|---|---|---|---|
| 2.8 | 28.55 | 23.6 | 0.47 |
| 3 | 30 | 26.1 | 0.45 |
| 4 | 39 | 37.6 | 0.365 |
| 5 | 48.5 | 29.9 | 0.36 |
| 10 | 70 | 28 | 0.654 |
| 15 | 115 | 56 | 0.717 |
| 20 | 139 | 88 | 0.734 |
| 25 | 163.9 | 268 | 0.353 |
| 30 | 212.31 | 351 | 0.397 |
| 35 | 256.4 | 295 | 0.423 |

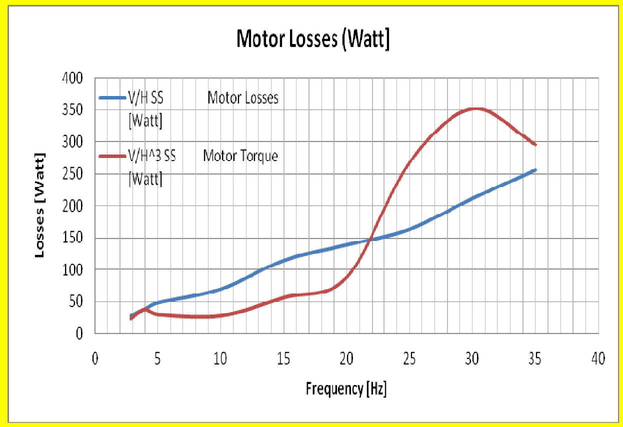


TABLE 8: NET SAVING IN PUMPING SYSTEM POWER

| Freq [Hz] | Reduction in Motor Input Power | Increase in Motor Output Power | Increase in Pump Input Power | Net saving in Pumping Power |
|---|---|---|---|---|
| 2.8 | 5 | 0.05 | 0.02 | 4.93 |
| 3 | 4 | 0.1 | 0.02 | 3.88 |
| 4 | 1.5 | 0.1 | 0.02 | 1.38 |
| 5 | 19 | 0.4 | 0.45 | 18.15 |
| 10 | 54 | 12 | 6 | 36 |
| 15 | 94 | 35 | 25 | 34 |
| 20 | 117 | 66 | 50 | 1 |
| 25 | 124.1 | 20 | 18 | 86.1 |
| 30 | 182.69 | 44 | 32 | 106.69 |
| 35 | 63.6 | 25 | 17 | 21.6 |

Analyzing the Power results, it was found that the reduction in the "Motor Input Power" along the frequency range is more effective than the increase in "Motor Output Power" and "Pump Output Power". Table 8 illustrates the Net saving in pumping system power that causes the improvement of the pumping system efficiency, where:

$$\text{Efficiency} = \text{Pump Output Power} / \text{Motor Input Power} \quad (10)$$

Since the reduction in the Motor Input power is more than the increase of the Pump Out put power, so the resultant efficiency is increased.

*D.Speed*

Table 9 summarizes the speed of the pump-motor results from applying the V/Hz and V/Hz$^3$ controllers. A slight different in the speed is observed between operating the motor with V/H control and V/Hz$^3$ control. This slight change in the speed is actually due to the change in the applied voltage that causes slight change in the operating torque value, and normally this do not result effective change in the speed of the Induction motors.

TABLE 9: MOTOR-PUMP SPEED

| Freq [Hz] | V/H SS RPM | V/H^3 SS RPM | MAX % Efficiency |
|---|---|---|---|
| 2.8 | 53 | 53 | 0.47 |
| 3 | 57.5 | 57.5 | 0.45 |
| 4 | 77.2 | 77.2 | 0.365 |
| 5 | 97.2 | 96.2 | 0.36 |
| 10 | 195 | 181 | 0.654 |
| 15 | 294.8 | 274.7 | 0.717 |
| 20 | 393.4 | 371.9 | 0.734 |
| 25 | 491.3 | 495.3 | 0.353 |
| 30 | 589.5 | 595 | 0.397 |
| 35 | 688.5 | 691 | 0.423 |

*E. Starting Current:*

Starting current time for the motor based on V/Hz characteristic is shown in the Figure 13. This data is important for the motor protection, as it can indicate the locked rotor case at different frequencies. Accordingly, the protective relay has to be programmed to initiate tripping signal in case the actual starting time of the motor exceeds the starting time given in (Fig.13).

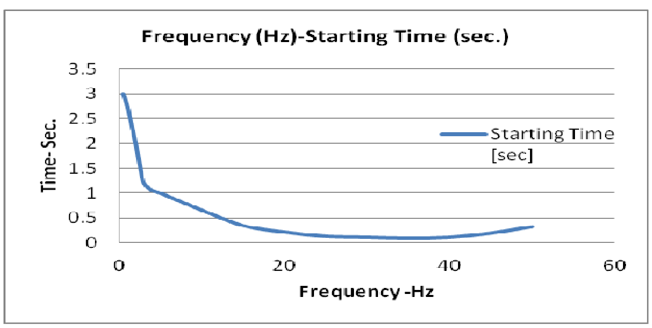


Figure 13: Comparison Motor Starting Time Results

## IV. CONCLUSION

The proposed closed loop fuzzy controller presented in this paper shows an efficient, fast and accurate technique in motor control. As seen from the overall structure of the controller, it utilizes both V/Hz and V/Hz$^3$ characteristics to achieve maximum efficiency for energy pumped storage system. Better efficiency has been achieved by using full wave Thyristor circuit control instead of DC link to control the voltage-frequency dependent characteristics. The effective reason that causes the improvement of the efficiency is the improvement of the motor power factor. This paper will bring the attention in the future work towards generalizing the motor controllers to include both V/Hz and V/Hz$^3$ characteristics so that the optimum voltage frequency dependent characteristic can be selected to achieve the minimum losses and maximum efficiency of the motor. Several issues - also need to be considered in the future such as the harmonics issue by describing a harmonics filter. In addition to that, protection relays setting need to be checked during the controller action.

ACKNOWLEDGMENT

I'd like to thank and pry to my Mother for her continuous support, care and pray during the preparation of this paper. This is the minimum gift that I can offer to admit her great role in my life. Also, I'd like to present my efforts to my sons Ahmed and Kareem and to my daughter Noor to encourage them for more learning efforts for better future.

## REFERENCES:

[1] E. Vittal, M. O'Malley, A. Keane, "A steady state voltage stability analysis of power systems with high penetration of wind," Trans of Power Systems, vol. 25, pp. 443-442, 2009.
[2] C. Bueno, J. Carta, "Wind powered pumped hydro storage systems, a means of increasing the penetration of renewable energy in the Canary Islands," Renewable and Sustainable Energy Reviews, vol. 10, pp. 312-340, 2006.
[3] D. Katsaprakakis, D. Christakis, A. Zervos, D. Papantonis, S. Voutsinas, "Pumped storage systems introduction in isolated power production systems," Renewable energy, vol. 33, issue 3, pp. 467-490,March, 2008.
[4] C. Cristofari, G. Notton, P. Philippe, M. Musselli, N. Herand, S. Nedelcheva, "Coupling hydro and wind electricity production by water – pumping storage," Proc. of first International Symposium on Environment Identities and Mediterranean Area, pp. 196-199, France, (2006).
[5] S. A. Papathanassiou, M. Tziantzi, M. P. Papadopoulos, S.T. Tentzerakis, P.S. Vionis, "Possible benefits from the combined operation of wind parks and pumped storage stations," Proc. Of European Wind Energy Conference and Exhibition, Madrid, Spain,2003.
[6] S. P. Mansoor, D. I. Jones, D.A. Bradley, F. C. Aris, "Stability of a pumped storage hydro power station connected to a power system," IEEE Engineering Society Winter Meeting, vol. 1, pp. 646-650, 1999.
[7] R. Peters, L. O'Malley, "Storing renewable power," Second Primer in the series: Making Renewable Energy a Priority, 2008.
[8] S. Papaefthymiou, E. Karamanou, S. Papathanassiou, M. Papadapoulos, "A wind hydro pumped storage station leading to high RES penetration in the autonomous island system of Ikaria," IEEE Transaction on Sustainable Energy, vol. 1, no. 3, October, 2010, pp. 163-172.
[9] A. Forcos, C. Marinescu, "A small autonomous system for storing wind energy by pumping water," Bulletin of the Polytechnic Institute of Iasi, in press, 2010.
[10] A. Forcos, C. Marinescu, "Motor Pump Group Efficiency in a Wind Energy Pumped Storage System" Advanced Topics in Electrical Engineering (ATEE), 2011 7th International Symposium, 12-14 May 2011
[11] Muhammad Harunur Rashid, Power Electronics Circuit, Devices and Applications, Prentice Hall Inc, NJ, 1988.
[12] MATLAB Software 6, SIMULINK manual, The MathWorks, Inc. 2001

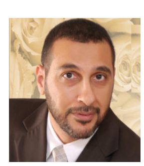

**Mohamed MAS Mahmoud** , Member of IEEE in 1999 and Senior Member (SM) in 2001.. Received the B.S. degree in Electrical Engineering from Cairo University and the M.Sc. degree from Kuwait University. He is currently PH.D researcher in Transilvania University of Brasov, Romania He occupies a position of Senior Engineer at Al Hosn Gas Co. His current research interests in Fuzzy and Artificial Neural Network Techniques application include power delivery, protection reliability, control and safety.